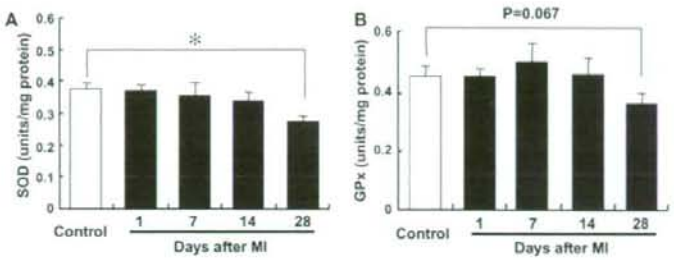

Figure 4. Time-dependent changes of activities of SOD (A) and GPx (B) in non-infarcted myocardium from sham-operated control ($n=7$) and on day 1 ($n=6$), day 7 ($n=10$), day 14 ($n=9$) and day 28 ($n=8$) after MI. Values are means ± SEM. * $p<0.05$ compared with sham-operated control.

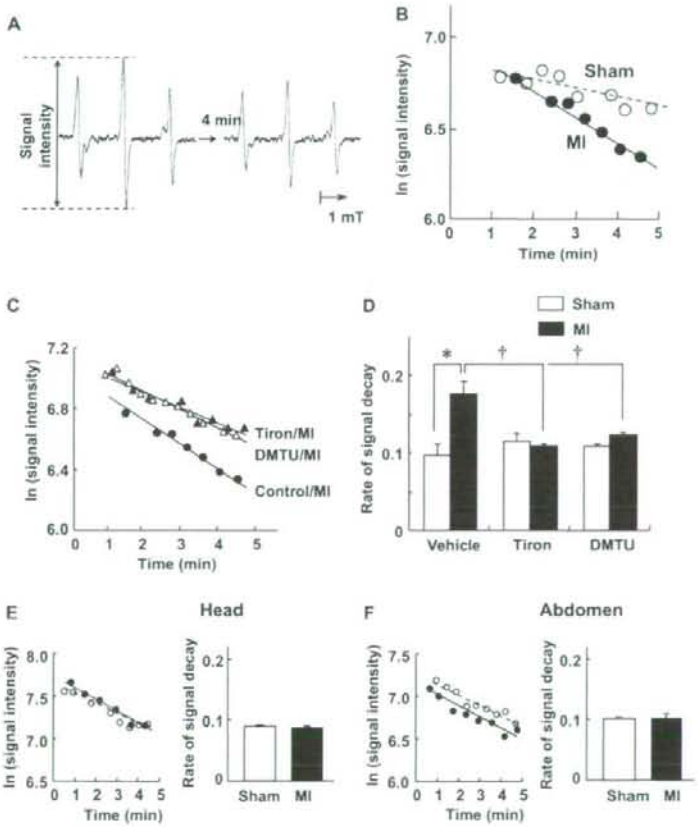

Figure 5. (A) A representative ESR signal of methoxycarbonyl-PROXYL at the chest level of a mouse with myocardial infarction (MI). (B) Semilogarithmic plots of the peak heights of the ESR spectra of methoxycarbonyl-PROXYL after spin probe injection. The signal intensity declined with time, which is defined as the signal decay. (C) The effects of addition of free radical scavengers on the rate of signal decay measured by *in vivo* ESR spectroscopy in individual MI mice. Tiron (a superoxide scavenger) or dimetylthiourea (DMTU; a hydroxyradical scavenger) was injected simultaneously with the injection of methoxycarbonyl-PROXYL. (D) Rates of signal decay measured by *in vivo* ESR in sham and MI groups in the absence and presence of radical scavengers ($n=6$ in each group). *$p<0.01$ vs sham-vehicle group and †$p<0.01$ vs MI-vehicle group. Values are means ± SEM. (E, F) Representative plots of individual mice and rates of *in vivo* ESR signal decay in sham and MI groups ($n=5$ each) measured at the head (E) and abdomen (F).

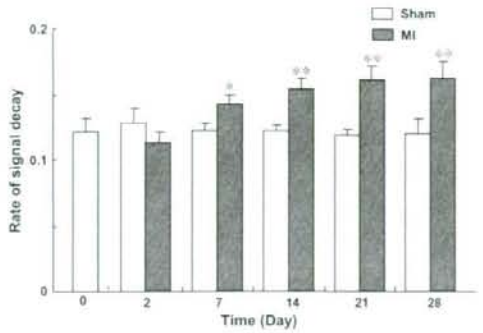

Figure 6. Changes in the rates of signal decay over time measured by *in vivo* ESR spectroscopy in sham and MI mice at days 0, 2, 7, 14 and 28 after operation ($n=7$ in each group). Values are means ±SEM. $^{*}p<0.05$, $^{**}p<.01$ vs sham values for the rate of signal decay.

peroxide, products of protein modifications and DNA damage do not always represent the net capacity of ROS reactions and do not necessary reflect ROS generation in specific organs or tissue. Difficulty in the interpretation of enhanced signal decay has been pointed out, because the nitroxyl radicals are known to react with not only free radicals but also other reductants including ascorbic acid and glutathione. However, we found that the increased ESR signal decay in heart failure was normalized by the addition of Tiron and DMTU. Furthermore, the TBARs study provided evidence that the ESR data reflect the increase of ROS in the failing heart, all of which support that the enhancement of signal decay in late remodelling represents at least the alteration of total redox status in the myocardium, most probably due to an increase of ROS.

Alteration of antioxidants and lipid peroxidation in non-infarct myocardium

We found that ROS markers including both byproducts of ROS and antioxidant enzymes were altered concomitantly in urine and blood at the early phase after MI and were normalized at the late remodelling state at 28 days post-MI. An increase of lipid peroxidation indicated by TBARS in infarct myocardium coincided with these systemic alterations (Figures 1 and 2). On the contrary, with the progression of remodelling represented by LV dilatation and reduced ejection fraction, the TBARS level in non-infarct myocardium increased at day 28. The immunohistochemical analysis by HEL antigen substantiated the finding that ROS was increased in the non-infarct myocardium during late remodelling. It is consistent with our previous findings in a tachycardia-induced canine HF model, in which ROS generation was enhanced in the failing myocardium and correlated with LV end-diastolic pressure and LV ejection fraction [41]. Nevertheless, it remains unknown why oxidative stress was not detectable in urine or in blood in late remodelling after MI, even with the progression of remodelling. A possible explanation is the differences in the source and amount of ROS between the early phase and the chronic phase of HF. In the later phase of post-MI remodelling, ROS increase may occur mainly in the myocardium and multiple defense mechanisms against ROS stabilize the levels in blood and urine. Moreover, ROS is so short-lived that it may not be possible to detect them in urine or blood when the source is localized in a single organ. In contrast, systemic inflammatory responses manifested clinically as leukocytosis and increased cytokines during acute deterioration or sudden ischemia [42–46] may not have enough time to cope with the acute ROS attack and redox change. We suspect that the acute increase in systemic ROS markers after MI is due to systemic activation of inflammatory cells. However, while administration of cyclophosphamide depletes leukocytes by 93% [15,47], the drug inhibited TBARS only partially by ~ 48% (data not shown). This indicates that sources other than leukocytes, such as vasculature, may contribute to systemic ROS generation in the acute phase of MI. All of these results suggest the difficulties of detecting ROS in blood or urine by specific markers in chronic HF, even with enhanced production of ROS from the remodelling myocardium.

Among the many detection techniques of ROS markers available currently, the most sensitive method is the detection of isoprostanes by mass spectroscopy. However, it is known that most of the major peaks of isoprostanes are not elevated in urine from HF patients [30]. Furthermore, commercially available ELISA kits are not as reliable as GC-MS assay [48]. Therefore, we measured a sensitive but not very specific marker TBARS for estimating ROS in plasma.

Clinical implications

Our study suggests that the increased local production of ROS is not always reflected in blood or urine during progression of remodelling. ROS are extremely unstable and difficult to detect directly. The establishment of a non-invasive method to detect ROS generated locally in the remodelling myocardium may permit time- and tissue-targeted therapy for more effective treatment of remodelling and failing heart.

Conclusion

We demonstrated that the generation of ROS in the non-infarct myocardium increases with the progression of cardiac remodelling and this increase is not

reflected by the levels of ROS markers in blood and urine. Clarification of the mechanisms of ROS-mediated remodelling and targeting non-infarct myocardium may lead to novel and effective therapeutic strategies for HF.

Acknowledgements

This study was supported in part by the Uehara memorial foundation and grants from the Ministry of Education (181-00006). A part of this study was conducted in Kyushu University Station for Collaborative Research II.

***Declaration of interest*:** The authors report no conflicts of interest. The authors alone are responsible for the content and writing of the paper.

References

[1] Gheorghiade M, Bonow RO. Chronic heart failure in the United States: a manifestation of coronary artery disease. Circulation 1998;97:282–289.

[2] Cohn JN, Ferrari R, Sharpe N. Cardiac remodeling—concepts and clinical implications: a consensus paper from an international forum on cardiac remodeling. Behalf of an International Forum on Cardiac Remodeling. J Am Coll Cardiol 2000;35:569–582.

[3] Liew CC, Dzau VJ. Molecular genetics and genomics of heart failure. Nat Rev Genet 2004;5:811–825.

[4] Tsutsui H, Ide T, Hayashidani S, Kinugawa S, Suematsu N, Utsumi H, Takeshita A. Effects of ACE inhibition on left ventricular failure and oxidative stress in Dahl salt-sensitive rats. J Cardiovasc Pharmacol 2001;37:725–733.

[5] Ichihara S, Yamada Y, Ichihara G, Kanazawa H, Hashimoto K, Kato Y, Matsushita A, Oikawa S, Yokota M, Iwase M. Attenuation of oxidative stress and cardiac dysfunction by bisoprolol in an animal model of dilated cardiomyopathy. Biochem Biophys Res Commun 2006;350:105–113.

[6] Mollnau H, Oelze M, August M, Wendt M, Daiber A, Schulz E, Baldus S, Kleschyov AL, Materne A, Wenzel P, Hink U, Nickenig G, Fleming I, Munzel T. Mechanisms of increased vascular superoxide production in an experimental model of idiopathic dilated cardiomyopathy. Arterioscler Thromb Vasc Biol 2005;25:2554–2559.

[7] Shite J, Qin F, Mao W, Kawai H, Stevens SY, Liang C. Antioxidant vitamins attenuate oxidative stress and cardiac dysfunction in tachycardia-induced cardiomyopathy. J Am Coll Cardiol 2001;38:1734–1740.

[8] Carlberg I, Mannervik B. Purification and characterization of the flavoenzyme glutathione reductase from rat liver. J Biol Chem 1975;250:5475–5480.

[9] Ide T, Tsutsui H, Kinugawa S, Suematsu N, Hayashidani S, Ichikawa K, Utsumi H, Machida Y, Egashira K, Takeshita A. Direct evidence for increased hydroxyl radicals originating from superoxide in the failing myocardium. Circ Res 2000;86:152–157.

[10] Lang D, Mosfer SI, Shakesby A, Donaldson F, Lewis MJ. Coronary microvascular endothelial cell redox state in left ventricular hypertrophy: the role of angiotensin II. Circ Res 2000;86:463–469.

[11] Kinugawa S, Tsutsui H, Hayashidani S, Ide T, Suematsu N, Satoh S, Utsumi H, Takeshita A. Treatment with dimethylthiourea prevents left ventricular remodeling and failure after experimental myocardial infarction in mice: role of oxidative stress. Circ Res 2000;87:392–398.

[12] Shiomi T, Tsutsui H, Matsusaka H, Murakami K, Hayashidani S, Ikeuchi M, Wen J, Kubota T, Utsumi H, Takeshita A. Overexpression of glutathione peroxidase prevents left ventricular remodeling and failure after myocardial infarction in mice. Circulation 2004;109:544–549.

[13] Matsushima S, Kinugawa S, Ide T, Matsusaka H, Inoue N, Ohta Y, Yokota T, Sunagawa K, Tsutsui H. Overexpression of glutathione peroxidase attenuates myocardial remodeling and preserves diastolic function in diabetic heart. Am J Physiol Heart Circ Physiol 2006;291:H2237–H2245.

[14] Suematsu N, Tsutsui H, Wen J, Kang D, Ikeuchi M, Ide T, Hayashidani S, Shiomi T, Kubota T, Hamasaki N, Takeshita A. Oxidative stress mediates tumor necrosis factor-alpha-induced mitochondrial DNA damage and dysfunction in cardiac myocytes. Circulation 2003;107:1418–1423.

[15] Machida Y, Kubota T, Kawamura N, Funakoshi H, Ide T, Utsumi H, Li YY, Feldman AM, Tsutsui H, Shimokawa H, Takeshita A. Overexpression of tumor necrosis factor-alpha increases production of hydroxyl radical in murine myocardium. Am J Physiol Heart Circ Physiol 2003;284:H449–H455.

[16] Foo RS, Siow RC, Brown MJ, Bennett MR. Heme oxygenase-1 gene transfer inhibits angiotensin II-mediated rat cardiac myocyte apoptosis but not hypertrophy. J Cell Physiol 2006;209:1–7.

[17] Nakagami H, Takemoto M, Liao JK. NADPH oxidase-derived superoxide anion mediates angiotensin II-induced cardiac hypertrophy. J Mol Cell Cardiol 2003;35:851–859.

[18] Siwik DA, Chang DL, Colucci WS. Interleukin-1beta and tumor necrosis factor-alpha decrease collagen synthesis and increase matrix metalloproteinase activity in cardiac fibroblasts *in vitro*. Circ Res 2000;86:1259–1265.

[19] Siwik DA, Pagano PJ, Colucci WS. Oxidative stress regulates collagen synthesis and matrix metalloproteinase activity in cardiac fibroblasts. Am J Physiol Cell Physiol 2001;280:C53–C60.

[20] Matsushima S, Ide T, Yamato M, Matsusaka H, Hattori F, Ikeuchi M, Kubota T, Sunagawa K, Hasegawa Y, Kurihara T, Oikawa S, Kinugawa S, Tsutsui H. Overexpression of mitochondrial peroxiredoxin-3 prevents left ventricular remodeling and failure after myocardial infarction in mice. Circulation 2006;113:1779–1786.

[21] Pimentel DR, Amin JK, Xiao L, Miller T, Viereck J, Oliver-Krasinski J, Baliga R, Wang J, Siwik DA, Singh K, Pagano P, Colucci WS, Sawyer DB. Reactive oxygen species mediate amplitude-dependent hypertrophic and apoptotic responses to mechanical stretch in cardiac myocytes. Circ Res 2001;89:453–460.

[22] Shiomi T, Tsutsui H, Hayashidani S, Suematsu N, Ikeuchi M, Wen J, Ishibashi M, Kubota T, Egashira K, Takeshita A. Pioglitazone, a peroxisome proliferator-activated receptor-gamma agonist, attenuates left ventricular remodeling and failure after experimental myocardial infarction. Circulation 2002;106:3126–3132.

[23] Yamamoto Y, Takahashi K. Glutathione peroxidase isolated from plasma reduces phospholipid hydroperoxides. Arch Biochem Biophys 1993;305:541–545.

[24] Sano H, Matsumoto K, Utsumi H. Synthesis and imaging of blood-brain-barrier permeable nitroxyl-probes for free radical reactions in brain of living mice. Biochem Mol Biol Int 1997;42:641–647.

[25] Han JY, Takeshita K, Utsumi H. Noninvasive detection of hydroxyl radical generation in lung by diesel exhaust particles. Free Radic Biol Med 2001;30:516–525.

[26] Phumala N, Ide T, Utsumi H. Noninvasive evaluation of *in vivo* free radical reactions catalyzed by iron using *in vivo* ESR spectroscopy. Free Radic Biol Med 1999;26:1209–1217.
[27] Belch JJ, Bridges AB, Scott N, Chopra M. Oxygen free radicals and congestive heart failure. Br Heart J 1991;65:245–248.
[28] Dieterich S, Bieligk U, Beulich K, Hasenfuss G, Prestle J. Gene expression of antioxidative enzymes in the human heart: increased expression of catalase in the end-stage failing heart. Circulation 2000;101:33–39.
[29] Ide T, Tsutsui H, Hayashidani S, Kang D, Suematsu N, Nakamura K, Utsumi H, Hamasaki N, Takeshita A. Mitochondrial DNA damage and dysfunction associated with oxidative stress in failing hearts after myocardial infarction. Circ Res 2001;88:529–535.
[30] Cargnoni A, Ceconi C, Bernocchi P, Boraso A, Parrinello G, Curello S, Ferrari R. Reduction of oxidative stress by carvedilol: role in maintenance of ischaemic myocardium viability. Cardiovasc Res 2000;47:556–566.
[31] Guo P, Nishiyama A, Rahman M, Nagai Y, Noma T, Namba T, Ishizawa M, Murakami K, Miyatake A, Kimura S, Mizushige K, Abe Y, Ohmori K, Kohno M. Contribution of reactive oxygen species to the pathogenesis of left ventricular failure in Dahl salt-sensitive hypertensive rats: effects of angiotensin II blockade. J Hypertens 2006;24:1097–1104.
[32] Miwa S, Toyokuni S, Nishina T, Nomoto T, Hiroyasu M, Nishimura K, Komeda M. Spaciotemporal alteration of 8-hydroxy-2'-deoxyguanosine levels in cardiomyocytes after myocardial infarction in rats. Free Radic Res 2002;36:853–858.
[33] Zhang GX, Kimura S, Nishiyama A, Shokoji T, Rahman M, Yao L, Nagai Y, Fujisawa Y, Miyatake A, Abe Y. Cardiac oxidative stress in acute and chronic isoproterenol-infused rats. Cardiovasc Res 2005;65:230–238.
[34] Li H, Lawson JA, Reilly M, Adiyaman M, Hwang SW, Rokach J, FitzGerald GA. Quantitative high performance liquid chromatography/tandem mass spectrometric analysis of the four classes of F(2)-isoprostanes in human urine. Proc Natl Acad Sci USA 1999;96:13381–13386.
[35] Agnoletti L, Curello S, Bachetti T, Malacarne F, Gaia G, Comini L, Volterrani M, Bonetti P, Parrinello G, Cadei M, Grigolato PG, Ferrari R. Serum from patients with severe heart failure downregulates eNOS and is proapoptotic: role of tumor necrosis factor-alpha. Circulation 1999;100:1983–1991.
[36] Kunsch C, Medford RM. Oxidative stress as a regulator of gene expression in the vasculature. Circ Res 1999;85:753–766.
[37] Al-Mehdi AB, Zhao G, Dodia C, Tozawa K, Costa K, Muzykantov V, Ross C, Blecha F, Dinauer M, Fisher AB. Endothelial NADPH oxidase as the source of oxidants in lungs exposed to ischemia or high K+. Circ Res 1998;83:730–737.
[38] Iuchi T, Akaike M, Mitsui T, Ohshima Y, Shintani Y, Azuma H, Matsumoto T. Glucocorticoid excess induces superoxide production in vascular endothelial cells and elicits vascular endothelial dysfunction. Circ Res 2003;92:81–87.
[39] Bertuglia S, Giusti A. Microvascular oxygenation, oxidative stress, NO suppression and superoxide dismutase during postischemic reperfusion. Am J Physiol Heart Circ Physiol 2003;285:H1064–H1071.
[40] Taniyama Y, Griendling KK. Reactive oxygen species in the vasculature: molecular and cellular mechanisms. Hypertension 2003;42:1075–1081.
[41] Aebi H. Catalase *in vitro*. Methods Enzymol 1984;105:121–126.
[42] Nakamura H, Takata S, Umemoto S, Matsuzaki M. Induction of left ventricular remodeling and dysfunction in the recipient heart following donor heart myocardial infarction: new insights into the pathological role of tumor necrosis factor-alpha from a novel heterotopic transplant-coronary ligation model. J Cardiol 2003;41:41–42.
[43] Maury CP. Monitoring the acute phase response: comparison of tumour necrosis factor (cachectin) and C-reactive protein responses in inflammatory and infectious diseases. J Clin Pathol 1989;42:1078–1082.
[44] Guillen I, Blanes M, Gomez-Lechon MJ, Castell JV. Cytokine signaling during myocardial infarction: sequential appearance of IL-1 beta and IL-6. Am J Physiol 1995;269:R229–R235.
[45] Basaran Y, Basaran MM, Babacan KF, Ener B, Okay T, Gok H, Ozdemir M. Serum tumor necrosis factor levels in acute myocardial infarction and unstable angina pectoris. Angiology 1993;44:332–337.
[46] Marx N, Neumann FJ, Ott I, Gawaz M, Koch W, Pinkau T, Schomig A. Induction of cytokine expression in leukocytes in acute myocardial infarction. J Am Coll Cardiol 1997;30:165–170.
[47] Fine PE. Implications of different study designs for the evaluation of acellular pertussis vaccines. Dev Biol Stand 1997;89:123–133.
[48] Pratico D, Lawson JA, Rokach J, FitzGerald GA. The isoprostanes in biology and medicine. Trends Endocrinol Metab 2001;12:243–247.

This paper was first published online on iFirst on 1 December 2008.

Journal of Cardiology (2008) 52, 79–85

ELSEVIER

JOURNAL of CARDIOLOGY
Official Journal of the Japanese College of Cardiology
www.elsevier.com/locate/jjcc

ORIGINAL ARTICLE

Beneficial effects of Waon therapy on patients with chronic heart failure: Results of a prospective multicenter study

Masaaki Miyata (MD, FJCC)[a], Takashi Kihara (MD)[a], Takuro Kubozono (MD)[a], Yoshiyuki Ikeda (MD)[a], Takuro Shinsato (MD)[a], Toru Izumi (MD, FJCC)[b], Masunori Matsuzaki (MD, FJCC)[c], Tetsu Yamaguchi (MD, FJCC)[d], Hiroshi Kasanuki (MD, FJCC)[e], Hiroyuki Daida (MD, FJCC)[f], Masatoshi Nagayama (MD)[g], Kazuhiro Nishigami (MD)[h], Kumiko Hirata (MD)[i], Koichi Kihara (MD)[j], Chuwa Tei (MD, FJCC)[a,*]

[a] *Department of Cardiovascular, Respiratory and Metabolic Medicine, Graduated School of Medicine, Kagoshima University, 8-35-1 Sakuragaoka, Kagoshima 890-8520, Japan*
[b] *Department of Cardiology, Kitasato University School of Medicine, Sagamihara, Japan*
[c] *Division of Cardiology, Department of Medicine and Clinical Science, Graduate School of Medicine, Yamaguchi University, Ube, Japan*
[d] *Department of Cardiovascular Center Medicine, Toranomon Hospital, Tokyo, Japan*
[e] *Department of Cardiology, Tokyo Women's Medical University, Tokyo, Japan*
[f] *Department of Cardiovascular Medicine, Juntendo University, Tokyo, Japan*
[g] *Department of Cardiology, Sakakibara Heart Institute, Tokyo, Japan*
[h] *Division of Cardiology, Saiseikai Kumamoto Hospital Cardiovascular Center, Kumamoto, Japan*
[i] *Division of Cardiology, Higashisumiyoshi Morimoto Hospital, Osaka, Japan*
[j] *Division of Cardiology, Fujimoto Hayasuzu Hospital, Miyakonojo, Japan*

Received 17 June 2008; accepted 3 July 2008
Available online 27 August 2008

KEYWORDS
Waon therapy;
Heart failure;
Treatment

Summary
Background: We conducted a prospective multicenter case–control study to confirm the clinical efficacy and safety of Waon therapy on chronic heart failure (CHF).
Methods: Patients ($n = 188$) with CHF were treated with standard therapy for at least 1 week, and then were randomized to Waon therapy ($n = 112$) or a control group ($n = 76$). All patients continued conventional treatment for an additional 2 weeks.

* Corresponding author. Tel.: +81 99 275 5316; fax: +81 99 275 5322.
E-mail addresses: miyatam@m3.kufm.kagoshima-u.ac.jp (M. Miyata), tei@m.kufm.kagoshima-u.ac.jp (C. Tei).

doi:10.1016/j.jjcc.2008.07.009

Natriuretic peptides;
Brain;
Non-pharmacological therapy

The Waon therapy group was treated daily with a far infrared-ray dry sauna at 60 C for 15 min and then kept on bed rest with a blanket for 30 min for 2 weeks. Chest radiography, echocardiography, and plasma levels of brain natriuretic peptide (BNP) were measured before and 2 weeks after treatment.

Results: NYHA functional class significantly decreased after 2 weeks of treatment in both groups. Chest radiography also showed a significant decrease of the cardiothoracic ratio in both groups (Waon therapy: $57.2 \pm 8.0\%$ to $55.2 \pm 8.0\%$, $p < 0.0001$; control: $57.0 \pm 7.7\%$ to $56.0 \pm 7.1\%$, $p < 0.05$). Echocardiography demonstrated that left ventricular diastolic dimension (LVDd), left atrial dimension (LAD), and ejection fraction (EF) significantly improved in the Waon therapy group (LVDd: 60.6 ± 7.6 to 59.1 ± 8.4 mm, $p < 0.0001$; LAD: 45.4 ± 9.3 mm to 44.1 ± 9.4 mm, $p < 0.05$; EF: $31.6 \pm 10.4\%$ to $34.6 \pm 10.6\%$, $p < 0.0001$), but not in the control group (LVDd: 58.4 ± 10.3 mm to 57.9 ± 10.4 mm; LAD: 46.3 ± 9.7 mm to 46.2 ± 10.1 mm; EF: $36.6 \pm 14.1\%$ to $37.3 \pm 14.0\%$). The plasma concentration of BNP significantly decreased with Waon therapy, but not in the control group (Waon: 542 ± 508 pg/ml to 394 ± 410 pg/ml, $p < 0.001$; control: 440 ± 377 pg/ml to 358 ± 382 pg/ml).

Conclusion: Waon therapy is safe, improves clinical symptoms and cardiac function, and decreases cardiac size in CHF patients. Waon therapy is an innovative and promising therapy for patients with CHF.

Introduction

Chronic heart failure (CHF) is a major and growing public health problem in Japan, as in other developed countries. Drugs that interfere with excessive activation of the rennin–angiotensin–aldosterone system can relieve the symptoms of heart failure in patients with a depressed ejection fraction (EF) by stabilizing and/or reversing cardiac remodeling. Thus, angiotensin-converting enzyme (ACE) inhibitors, angiotensin II receptor blockers (ARBs), and β blockers have emerged as cornerstones of modern heart failure therapy for patients with a depressed EF [1]. Angiotensin II plays an important role in the pathogenesis of CHF, and many large clinical trials have demonstrated the benefits of ACE inhibitors [2,3], and ARBs [4–8] on the morbidity and mortality of CHF. However, the number of heart failure deaths has increased steadily despite advances in treatment, in part, because of increasing numbers of patients with CHF due to better treatment and salvage of patients with acute myocardial infarction earlier in life [9].

We developed a form of thermal therapy that differs from the traditional sauna [10], and have been investigating the effects of thermal therapy since 1989. We discovered that the new thermal therapy offers prominent beneficial effects for patients with CHF [10–13] and peripheral artery disease [14,15]. Thermal therapy at very high temperature was originally used to treat localized cancer. However, the therapy we developed to treat cardiovascular diseases is quite different, in that it consists of systemic soothing warmth that comfortably refreshes the mind and body. Therefore, we have changed the name from thermal, to "Waon" therapy, since "Waon" in Japanese means soothing warmth [16]. Waon therapy is defined as "therapy in which the entire body is warmed in an evenly heated chamber for 15 min at a temperature that soothes the mind and body, and after the deep-body temperature has increased by approximately 1.0–1.2 °C, the soothing warmth is sustained by maintaining the warmth at rest for an additional 30 min, with fluids supplied at the end to replace the loss from perspiration" [16]. We have reported that Waon therapy, the repeated use of a dry sauna at 60 °C, improves hemodynamics and ameliorates symptoms, suppresses ventricular arrhythmias, and improves vascular function in CHF patients [10–13]. We have already performed Waon therapy in several hundred CHF patients in our hospital without any severe adverse effects.

In order to expand the use of Waon therapy, we developed a movable and sitting-position sauna system, in which the temperature at the top and bottom of the chamber is uniformly maintained at the same temperature of 60 °C (Fig. 1). Using this sitting-position sauna system, we conducted a prospective multicenter case–control study to confirm the clinical effect and safety of Waon therapy on CHF at 10 different hospitals.

Subjects and methods

Subjects

Ten hospitals participated in this multicenter study: Kagoshima University Hospital, Kitasato University Hospital, Sakakibara Memorial Hospital, Yamaguchi University Hospital, Juntendo University Hospital, Tokyo Women's Medical University Hospital, Toranomon Hospital, Higashisumiyoshi Morimoto Hospital, Saiseikai Kumamoto Hospital, and Fujimoto Hayasuzu Hospital. We enrolled 188 patients with CHF, aged 26–94 years (mean age: 64.7 ± 13.7 years). 94 patients had idiopathic dilated cardiomyopathy, 45 had ischemic cardiomyopathy, 16 patients had valvular heart disease, and 33 patients had other heart disease (7 hypertensive heart disease, 10 hypertrophic cardiomyopathy, 4 dilated hypertrophic cardiomyopathy, 3 cardiac sarcoidosis, 3 restrictive cardiomyopathy, 2 atrial septal defect, 1 cardiac amyloidosis, 1 drug-induced cardiomyopathy, 1 alcoholic cardiomyopathy, and 1 left ventricular noncompaction).

Inclusion criteria were the presence of symptomatic CHF, left ventricular ejection fraction (LVEF) <50% on echocardiography, and New York Heart Association (NYHA) functional classes II–IV. Exclusion criteria were the presence of severe aortic stenosis, severe obstruction with hypertrophic obstructive cardiomyopathy, and high fever due to infectious disease. Informed consent was obtained from all of the patients before participation. This protocol was approved by the Ethics Committee of the Faculty of Medicine, Kagoshima University.

Design of the study protocol

All patients could receive any kind of medication for CHF and doctors also could change the medication during the study. The subjects were treated with conventional therapy for at least 1 week, and then were randomized to the Waon therapy group or a control group at each hospital. The patients in the Waon therapy group received thermal therapy daily, 5 days a week, for 2 weeks. The patients in the control group continued the conventional treatment for 2 more weeks.

Waon therapy

Waon therapy uses a far infrared-ray dry sauna, which is evenly maintained at 60 °C and differs from traditional sauna. Waon therapy has an absence of hydration pressure, and was performed as previously reported [10]. Briefly, the patients were placed in a sitting-position in a 60 °C sauna system for 15 min, and then after leaving the sauna, they underwent bed rest with a blanket to keep them warm for an additional 30 min. All patients were weighed before and after the therapy, and oral hydration with water was used to compensate for weight lost due to perspiration. Waon therapy was performed once a day, 5 days a week for 2 weeks, for a total of 10 sessions. To rule out any acute effects of Waon therapy, all examinations were performed before the first treatment and on the next day after the last treatment.

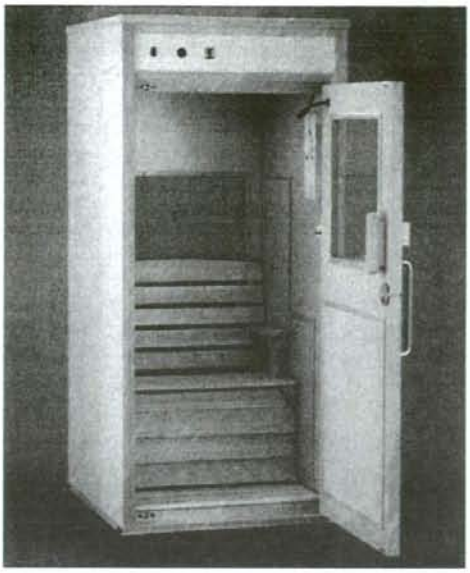

Figure 1 Movable and sitting-position sauna system. The temperature at the top and bottom of the chamber is uniformly maintained at the same temperature of 60 C.

Measurements

Physical examination

The blood pressure (BP), pulse rate, body weight, and body temperature were measured before and 2 weeks after treatment.

Cardiac function

The clinical state of CHF was evaluated by NYHA functional class. Before and 2 weeks after treatment, the cardiothoracic ratio (CTR) was measured by chest radiography and left ventricular diastolic dimension (LVDd), left atrial dimension (LAD), and

Table 1 Baseline clinical characteristics and changes in several variables

	Waon therapy group ($n=112$)			Control group ($n=76$)			Comparison at baseline[a]
	Baseline	After 2 weeks	p-Value	Baseline	After 2 weeks	p-Value	p-Value
Age (years)	63 ± 13			66 ± 14			NS
Gender (male/female)	74/38			51/25			NS
DCM/ICM/VD/other disease	62/29/7/14			32/16/9/19			NS
NYHA functional class (average)	2.61 ± 0.62	1.99 ± 0.60	<0.0001	2.51 ± 0.62	2.23 ± 0.48	<0.01	NS
Body weight (kg)	56.7 ± 11.8	55.9 ± 11.4	<0.0001	54.6 ± 12.5	54.6 ± 12.5	NS	NS
Heart rate (beats/min)	74 ± 15	72 ± 13	NS	74 ± 13	71 ± 11	NS	NS
Systolic BP (mm Hg)	108 ± 21	104 ± 18	<0.01	110 ± 21	106 ± 19	<0.05	NS
Diastolic BP (mm Hg)	64 ± 12	62 ± 11	<0.01	67 ± 12	65 ± 10	<0.05	NS

DCM, dilated cardiomyopathy; ICM, ischemic cardiomyopathy; VD, valvular disease; NYHA, New York Heart Association; BP, blood pressure; and NS, not significant.
[a] Comparison with baseline values. Data are presented as the mean value ± S.D.

LVEF were evaluated by conventional echocardiography.

Laboratory measurements

A fasting blood sample was obtained in the morning to measure the plasma concentrations of the brain natriuretic peptide (BNP) with radioimmunoassay, before and 2 weeks after treatment.

Statistical analysis

All data are expressed as the mean value ± S.D. Differences in baseline characteristics were evaluated by a χ^2 test and unpaired t-test. The data before and 2 weeks after treatment were compared using a paired t-test. A p-value of <0.05 was considered statistically significant.

Results

Baseline clinical characteristics

The baseline clinical characteristics are summarized in Table 1. There were no significant differences in age, gender, causative heart disease, NYHA functional class, body weight, heart rate, systolic BP (SBP), or diastolic BP (DBP) at baseline between the two groups.

Clinical findings and physical examinations

During the study, none of the patients treated with Waon therapy had worsened clinical symptoms. The changes in the clinical findings and variables after 2 weeks are summarized in Table 1. NYHA functional class, SBP, and DBP significantly decreased in both groups. Body weight significantly decreased in the Waon therapy group, but not in the control group. There were no significant changes in heart rate in either group.

Chest radiography and echocardiography

Fig. 2 shows the results of chest radiography and echocardiography. Chest radiography showed a significant decrease of the CTR after 2 weeks of treatment in both groups (Waon therapy group: 57.2 ± 8.0% to 55.2 ± 8.0%, $p<0.0001$; control group: 57.0 ± 7.7% to 56.0 ± 7.1%, $p<0.05$). In addition, echocardiography demonstrated that LVDd, LAD, and LVEF significantly improved after Waon therapy (LVDd: 60.6 ± 7.6 mm to 59.1 ± 8.4 mm, $p<0.0001$; LAD: 45.4 ± 9.3 mm to 44.1 ± 9.4 mm,

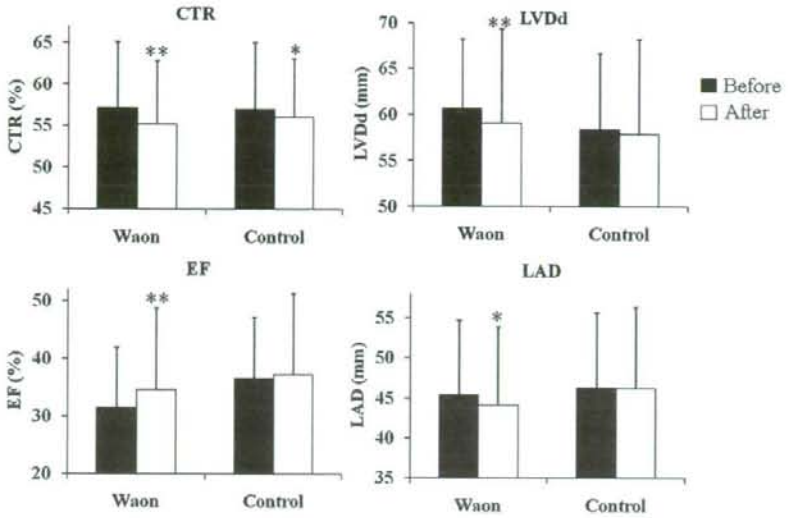

Figure 2 Data from chest radiography and echocardiography. Chest radiography showed a significant decrease of the cardiothoracic ratio (CTR) after 2 weeks of treatment in both groups. Echocardiography demonstrated that left ventricular diastolic dimension (LVDd), left atrial dimension (LAD), and left ventricular ejection fraction (LVEF) significantly decreased after 2 weeks of Waon therapy, but did not change after 2 weeks of conventional therapy in the control group. *$p < 0.05$ vs. baseline; **$p < 0.0001$ vs. baseline. Closed bars show baseline and open bars indicate values after 2 weeks of treatment.

$p < 0.05$; LVEF: $31.6 \pm 10.4\%$ to $34.6 \pm 10.6\%$, $p < 0.0001$), but did not change in the control group (LVDd: 58.4 ± 10.3 mm to 57.9 ± 10.4 mm, not significant; LAD: 46.3 ± 9.7 mm to 46.2 ± 10.1 mm, not significant; LVEF: $36.6 \pm 14.1\%$ to $37.3 \pm 14.0\%$, not significant).

Plasma levels of BNP

Fig. 3 shows the changes in plasma concentration of BNP. The plasma concentration of BNP significantly decreased after 2 weeks of Waon therapy, while it did not change in the control group (Waon therapy group: 542 ± 508 pg/ml to 394 ± 410 pg/ml, $p < 0.001$; control group: 440 ± 377 pg/ml to 358 ± 382 pg/ml, not significant).

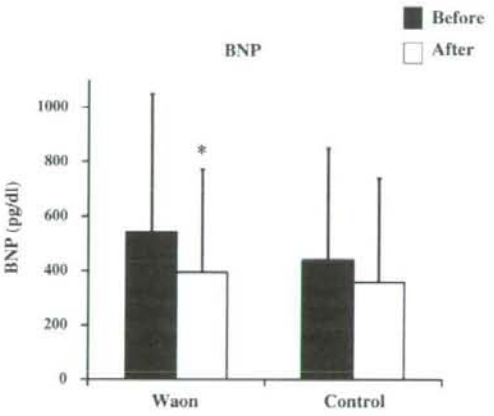

Figure 3 Changes in plasma concentration of BNP. The plasma concentration of BNP significantly decreased after 2 weeks of Waon therapy, but did not change in the control group. *$p < 0.001$ vs. baseline. Closed bars show baseline and open bars indicate values after 2 weeks of treatment.

Discussion

We developed the sitting-position sauna system, and conducted a prospective multicenter case–control study to confirm the clinical efficacy and safety of Waon therapy on CHF at 10 hospitals. In this study, we confirmed that Waon therapy improved clinical symptoms and cardiac function evaluated by echocardiography and BNP concentrations, and decreased cardiac size on chest radiography and echocardiography after 2 weeks of Waon therapy in patients with CHF. We also demonstrated that our movable and sitting-position sauna system is effective and safe for patients with CHF.

Regarding the acute effect of Waon therapy, we have reported that 60 °C sauna therapy for 15 min improved acute hemodynamics in patients with CHF, including cardiac index, mean pulmonary wedge pressure, systemic and pulmonary resistance, and cardiac function [10]. Subsequently, we examined the chronic effects of repeated Waon therapy on clinical symptoms and cardiac function in patients with CHF and have reported that 4 weeks of Waon therapy significantly improved clinical symptoms, increased ejection fraction, and decreased cardiac size on the echocardiogram and chest X-ray [10,11]. Furthermore, we demonstrated that daily Waon therapy for 2 weeks decreased ventricular premature contractions and increased heart rate variability (SDNN, standard deviation of normal-to-normal beat interval) in patients with CHF, suggesting that Waon therapy decreased sympathetic nervous activity and improved ventricular arrhythmias [13].

We then investigated the vascular endothelial function to clarify the mechanisms of the effect of Waon therapy on CHF, since vascular endothelial function had been reported to be impaired in CHF. We have reported that 2 weeks of Waon therapy significantly reduced BNP concentrations and improved endothelial function in patients with CHF. There was a significant correlation between the change in %FMD (flow-mediated dilatation) and the percent improvement in BNP concentrations in the Waon therapy group [12].

In order to confirm the effect of Waon therapy on CHF and clarify its mechanism, we performed experimental studies using TO-2 cardiomyopathic hamsters with heart failure. We reported that the repeated Waon therapy improved survival in TO-2 cardiomyopathic hamsters with heart failure [17]. We clarified that one of the molecular mechanisms by which repeated Waon therapy improved endothelial function was an increase in mRNA and protein of endothelial nitric oxide synthase (eNOS) in Syrian golden hamsters [18] and TO-2 cardiomyopathic hamsters [19]. We believe that eNOS up-regulation induced by repeated Waon therapy is caused by an increase in cardiac output and blood flow, which in turn results in increased shear stress, although thermal stimulation might up-regulate arterial eNOS directly.

Compared to pharmacological vasodilator therapy and other non-pharmacological therapy, such as cardiac resynchronization therapy and physical therapy, there are several advantages of Waon therapy for CHF. First, it is quite safe and has no adverse effects. Second, it is less expensive and more cost-effective. Third, unlike physical therapy, patients who are elderly or have severe congestive heart failure, uncontrolled ventricular arrhythmias, and orthopedic limitations are not exempt from undergoing Waon therapy. Fourth, this treatment promotes mental and physical relaxation. Waon therapy may thus be a valuable adjunct to pharmacological or non-pharmacological intervention in the management of CHF.

We have treated many CHF patients with Waon therapy, and none of the patients so far has shown any deterioration in their condition. However, Waon therapy does not appear to be indicated for CHF patients with severe aortic stenosis or obstructive hypertrophic cardiomyopathy, because the pressure gradient might be increased during Waon therapy. Patients with infectious disease are also excluded from Waon therapy.

Study limitations

We have already reported that repeated Waon therapy improved the prognosis of TO-2 cardiomyopathic hamsters with CHF, suggesting a new potential non-pharmacologic therapy for CHF [17]. The ultimate goal of treatment is the improvement of prognosis and quality of life. Therefore, we must evaluate the effect of Waon therapy on prognosis, as well as quality of life, in patients with CHF. We are conducting a prospective clinical randomized study to assess the impact of Waon therapy on the rate of cardiac death or re-hospitalization in patients with CHF.

Conclusion

In this prospective multicenter study, we confirmed that Waon therapy is quite safe, improved clinical symptoms and cardiac function, and decreased cardiac size in patients with CHF. Therefore, Waon therapy is an innovative and promising therapy for patients with CHF.

Acknowledgements

We appreciated Dr. Tsuyoshi Fukudome, Dr. Shoji Fujita, and Dr. So Kuwahata in Kagoshima University, Dr. Chiharu Noda in Kitasato University, Dr. Shigeki Kobayashi in Yamaguchi University, Dr. Katsuyuki Masaki in Juntendo University, Dr. Kazue Watanabe in Tokyo Women's Medical University, and Dr. Minoru Ohno in Toranomon Hospital for collecting data at each hospital.

References

[1] Mann DL. Management of heart failure patients with reduced ejection fraction. In: Libby P, Bonow RO, Mann DL, Zipes DP, editors. Braunwald's heart disease: a textbook of cardiovascular medicine. 8th ed. Philadelphia: WB Saunders; 2008. p. 611–40.

[2] The CONSENSUS Trial Study Group.Effects of enalapril on mortality in severe congestive heart failure. Results of the Cooperative North Scandinavian Enalapril Survival Study (CONSENSUS). N Engl J Med 1987;316:1429–35.

[3] The SOLVD Investigators.Effect of enalapril on survival in patients with reduced left ventricular ejection fractions and congestive heart failure. N Engl J Med 1991;325:293–302.

[4] Cohn JN, Tognoni G, Valsartan Heart Failure Trial Investigators. A randomized trial of the angiotensin-receptor blocker valsartan in chronic heart failure. N Engl J Med 2001;345:1667–75.

[5] Pfeffer MA, Swedberg K, Granger CB, Held P, McMurray JJ, Michelson EL, et al. Effects of candesartan on mortality and morbidity in patients with chronic heart failure: the CHARM-overall programme. Lancet 2003;362:759–66.

[6] McMurray JJ, Ostergren J, Swedberg K, Granger CB, Held P, Michelson EL, et al. Effects of candesartan in patients with chronic heart failure and reduced left-ventricular systolic function taking angiotensin-converting-enzyme inhibitors: the CHARM-added trial. Lancet 2003;362:767–71.

[7] Granger CB, McMurray JJ, Yusuf S, Held P, Michelson EL, Olofsson B, et al. Effects of candesartan in patients with chronic heart failure and reduced left-ventricular systolic function intolerant to angiotensin-converting-enzyme inhibitors: the CHARM-alternative trial. Lancet 2003;362:772–6.

[8] Yusuf S, Pfeffer MA, Swedberg K, Granger CB, Held P, McMurray JJ, et al. Effects of candesartan in patients with chronic heart failure and preserved left-ventricular ejection fraction: the CHARM-preserved Trial. Lancet 2003;362:777–81.

[9] Hunt SA, Abraham WT, Chin MH, Feldman AM, Francis GS, Ganiats TG, et al. American College of Cardiology; American Heart Association Task Force on Practice Guidelines; American College of Chest Physicians; International Society for Heart and Lung Transplantation; Heart Rhythm Society. ACC/AHA 2005 Guideline Update for the Diagnosis and Management of Chronic Heart Failure in the Adult: a report of the American College of Cardiology/American Heart Association Task Force on Practice Guidelines (Writing Committee to Update the 2001 Guidelines for the Evaluation and Management of Heart Failure): developed in collaboration with the American College of Chest Physicians and the International Society for Heart and Lung Transplantation: endorsed by the Heart Rhythm Society. Circulation 2005;112:e154–235.

[10] Tei C, Horikiri Y, Park JC, Jeong JW, Chang KS, Toyama Y, et al. Acute hemodynamic improvement by thermal vasodilation in congestive heart failure. Circulation 1995;91:2582–90.

[11] Tei C, Tanaka N. Thermal vasodilation as a treatment of congestive heart failure: a novel approach. J Cardiol 1996;27:29–30.

[12] Kihara T, Biro S, Imamura M, Yoshifuku S, Takasaki K, Ikeda Y, et al. Repeated sauna treatment improves vascular endothelial and cardiac function in patients with chronic heart failure. J Am Coll Cardiol 2002;39:754–9.

[13] Kihara T, Biro S, Ikeda Y, Fukudome T, Shinsato T, Masuda A, et al. Effects of repeated sauna treatment on ventricular arrhythmias in patients with chronic heart failure. Circ J 2004;68:1146–51.

[14] Tei C, Shinsato T, Kihara T, Miyata M. Successful thermal therapy for end-stage peripheral artery disease. J Cardiol 2006;47:163–4.

[15] Tei C, Shinsato T, Miyata M, Kihara T, Hamasaki S. Waon therapy improves peripheral arterial disease. J Am Coll Cardiol 2007;50:2169–71.

[16] Tei C. Waon therapy: soothing warmth therapy. J Cardiol 2007;49:301–4.

[17] Ikeda Y, Biro S, Kamogawa Y, Yoshifuku S, Kihara T, Minagoe S, et al. Effect of repeated sauna therapy on survival in TO-2 cardiomyopathic hamsters with heart failure. Am J Cardiol 2002;90:343–5.

[18] Ikeda Y, Biro S, Kamogawa Y, Yoshifuku S, Eto H, Orihara K, et al. Repeated thermal therapy upregulates arterial endothelial nitric oxide synthase expression in Syrian golden hamsters. Jpn Circ J 2001;65:434–8.

[19] Ikeda Y, Biro S, Kamogawa Y, Yoshifuku S, Eto H, Orihara K, et al. Repeated sauna therapy increases arterial endothelial nitric oxide synthase expression and nitric oxide production in cardiomyopathic hamsters. Circ J 2005;69:722–9.

Am J Physiol Cell Physiol 294: C957–C965, 2008.
First published January 23, 2008; doi:10.1152/ajpcell.00505.2007.

Specific knockdown of m-calpain blocks myogenesis with cDNA deduced from the corresponding RNAi

Michiyo Honda,[1] Fujiko Masui,[2] Nobuyuki Kanzawa,[1] Takahide Tsuchiya,[1] and Teruhiko Toyo-oka[2,3]

[1]*Department of Chemistry, Faculty of Science and Engineering, Sophia University, Tokyo;* [2]*Department of Organ Pathophysiology and Internal Medicine, University of Tokyo, Tokyo; and* [3]*Department of Molecular Cardiology, Division of Biofunctional Sciences, Tohoku University Bioengineering Organization (TUBERO), Sendai, Japan*

Submitted 25 October 2007; accepted in final form 19 January 2008

Honda M, Masui F, Kanzawa N, Tsuchiya T, Toyo-oka T. Specific knockdown of m-calpain blocks myogenesis with cDNA deduced from the corresponding RNAi. *Am J Physiol Cell Physiol* 294: C957–C965, 2008. First published January 23, 2008; doi:10.1152/ajpcell.00505.2007.—Fusion of mononuclear myoblast to multinucleated myotubes is crucial for myogenesis. Both μ- and m-calpain are ubiquitously expressed in most cells and are particularly abundant in muscle cells. Knockout of calpain-1 (catalytic subunit of μ-calpain) induced moderate platelet dysaggregation, preserving the normal development and growth, although knockout of calpain-2 (m-calpain) is lethal in mice. Therefore, there should be muscle-specific function of m-calpain per se. Previous methods lack direct evidence for the involvement of m-calpain, because the specific inhibitor to m-calpain has not been developed yet and the inhibition was less potent. Here, we show that screened RNA interference (RNAi) specifically blocked the m-calpain expression by 95% at both the protein and the activity levels. After transfection of adenovirus vector-mediated cDNA corresponding to the RNAi-induced short hairpin RNA, m-calpain in C_2C_{12} myoblasts was knocked down with no compensatory overexpression of μ-calpain or calpain-3. The specific knockdown strongly inhibited the fusion to multinucleated myotubes. In addition, the knockdown modestly blocked ubiquitous effects, including cell migration, cell spreading, and alignment of central stress fiberlike structures. These results may indicate that m-calpain requiring millimolar Ca^{2+} level for the full activation plays specific roles in myogenesis, independent of μ-calpain, and leave us challenging problems in the future.

RNA interference; muscle cell development; fusion; adenovirus vector

CALPAINS FORM A SUPERFAMILY of Ca^{2+}-activated cytosolic cysteine proteases widely distributed from mammals to invertebrates. The conventional calpains (μ- and m-calpain) are composed of heterodimer with each catalytic subunit, encoded by calpain-1 (*Capn*1) or calpain-2 (*Capn*2), and a common regulatory subunit encoded by calpain-4 (*Capn*4). Calpain activity is regulated by a variety of factors, including Ca^{2+}, phospholipids, the small subunit, an endogenous calpain-specific inhibitor peptide, calpastatin, autodigestion, and phosphorylation via the ERK/MAPK pathway (21, 40). Calpain family has been implicated in a large number of physiological processes, including cell spreading, cell migration, myoblast fusion, cell cycle, and apoptosis (21), and in various pathological processes, such as neuromuscular diseases, cardiac dysfunction, cataract, and diabetes (24, 27, 43, 50). Skeletal and cardiac muscles contain large amounts of μ- and m-calpain that may contribute to the progression of muscular dystrophy and/or advanced heart failure (12, 44, 48), although the lack of a specific inhibitor for each calpain has made verification of each role difficult.

Transgenic animals are of great use for uncovering the physiological function of novel proteins and clarifying the molecular mechanism of several diseases, developing a new strategy for treatment. The knockout mice are, however, limited by the resultant developmental effects, genetic compensation, and lack of specificity, not at the whole animal level but at the cellular and/or organ level. In the case of *Capn*2, the homozygous disruption of the gene showed preimplantation lethality, indicating that this protease is indispensable for early embryogenesis (16). Here, we used RNA interference (RNAi) to generate a specific knockdown of *Capn*2 at the cellular level. A major challenge in applying this technique in vitro or in vivo has been addressed by introducing the small interfering RNA (siRNA) and short hairpin RNA (shRNA) into primary cultures or into target cells of higher living organisms (18, 29, 47, 49).

We generated *Capn*2 knockdown of the skeletal myoblast cell line C_2C_{12}, using an efficient adenovirus-mediated RNAi (37), and demonstrated clear evidence that m-calpain is involved in fusion of myoblasts to myotubes, in addition to other aspects of myogenesis.

MATERIALS AND METHODS

Materials. Anti-m-calpain antibody was kindly supplied by Dr. H. Sorimachi, Tokyo Metropolitan Institute for Clinical Sciences. Anti-α-tubulin (clone DM 1A) and anti-vinculin (clone hVIN1) antibodies were purchased from Sigma (St. Louis, MO). Alexa Fluor 594-labeled phalloidin was from Molecular Probes, Invitrogen (Carlsbad, CA). All other reagents were from Sigma.

Cell culture. C_2C_{12} cells supplied from Riken Gene Bank (Tsukuba, Japan) were cultured in growth medium (GM), Dulbecco's modified Eagle's medium (DMEM) with 10% fetal bovine serum, as described previously (36). To promote differentiation from skeletal myoblasts to myotubes and myocytes, the medium was replaced by the differentiation medium (DM) containing 2% horse serum after the cultured cells became confluent in GM.

Virus-mediated gene silencing of Capn2 by RNA interference. The BLOCK-iT Adeno Expression System (Invitrogen) was used for creating a replication-incompetent adenovirus that transiently delivered a shRNA of *Capn*2 to C_2C_{12} for RNAi. Hairpin RNA was designed to target specific regions of mouse *Capn*2 (GenBank acces-

Address for reprint requests and other correspondence: T. Toyo-oka, Dept. of Molecular Cardiology, Div. of Biofunctional Sciences, Tohoku Univ. Bioengineering Organization (TUBERO), Sendai 980-8575, Japan (e-mail: toyooka-dmc@tubero.tohoku.ac.jp).

The costs of publication of this article were defrayed in part by the payment of page charges. The article must therefore be hereby marked "*advertisement*" in accordance with 18 U.S.C. Section 1734 solely to indicate this fact.

sion no. NM_009794) mRNA. A control with a scrambled sequence lacked homology to any known *Mus musculus* mRNAs.

We synthesized two sets of oligonucleotides (Invitrogen): shcapn2 (top, 5′-CACCGGACGAAGATTCAGAAATACCCGAAGGTATTTCTGAATCTTCGTCC-3′; bottom, 5′-AAAAGGACGAAGATTCAGAAATACCTTCGGGTATTTCTGAATCTTCGTCC-3′) and shSCR (top, 5′-CACCGCTACACAAATCAGCGATTTCGAAAAATCGCTGATTTGTGTAG-3′; bottom, 5′-AAAACTACACAAATCAGCGATTTTTCGAAATCGCTGATTTGTGTAGC-3′).

These oligonucleotides were annealed and cloned into pENTR/U6 vector according to the manufacturer's instructions. All clones were verified by direct sequencing. The U6 promoter, hairpin sequence, and terminator sequences were ligated into a pAd/BLOCK-it DEST vector. Adenovirus expression plasmids were digested with *Pac* I to expose the inverted terminal repeats and were transfected into the 293A producer cells with Lipofectamine 2000 (Invitrogen) to produce adenovirus stock. Amplified adenovirus was used to knock down calpain-2, and the enzyme expression was analyzed by Western blot and casein zymography for verification of the expression at the protein and activity levels, respectively.

Quantitative mRNA assay. The quantity of mRNA from cultured cells was measured with a branched DNA signal amplification assay (Quantigene High Volume bDNA Signal Amplification Kit; Panomics, Fremont, CA), following the manufacturer's instructions. The premises for this assay have been extensively described by Hartley and Klaassen (22).

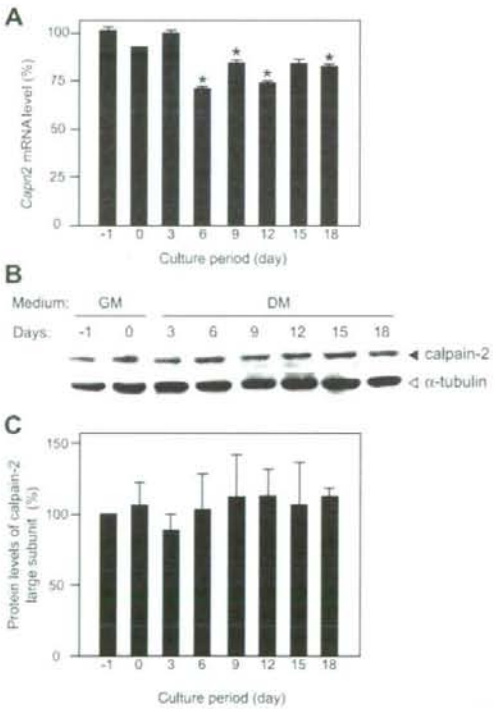

Fig. 1. Expressions of calpain-2 mRNA and protein in C_2C_{12}. *A*: mRNA levels of *Capn2* at different stages measured with the Quantigene system, as described in MATERIALS AND METHODS. Error bars indicate SEs. $^*P < 0.05$ by Student's *t*-test. *B*: Western blot analysis of full-length calpain-2 and α-tubulin (loading control). GM, growth medium; DM, differentiation medium. *C*: quantification of full-length calpain-2 protein levels at different stages. Error bars indicate SEs.

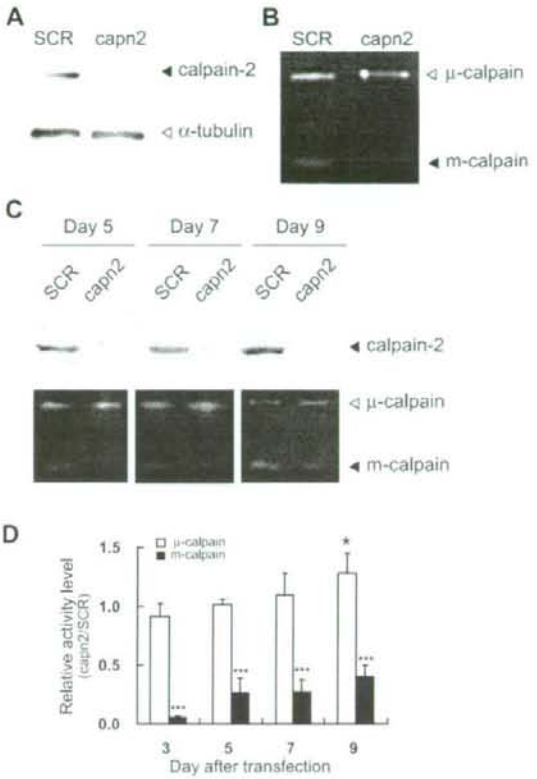

Fig. 2. Suppression of calpain-2 expression at protein and activity levels with adenovirus vector-mediated RNAi in C_2C_{12}. *A*: Western blotting of calpain-2 and α-tubulin at 3 days after transfection with Ad_shSCR (nonsilencing control; SCR) or Ad_shcapn2 (targeting calpain-2; capn2). *B*: zymography of 3-day posttransfection cells. *C*: sustained inhibition of calpain-2 from 5 to 9 days after transfection, analyzed with Western blotting (*top*) or zymography (*bottom*). *D*: comparison of relative activity levels of μ- and m-calpain in *Capn2* knockdown cells. The activities at *days 5*, *7*, and *9* were compared with the activity at *day 3*. Error bars indicate SEs. $^*P < 0.05$ and $^{***}P < 0.001$ by Student's *t*-test.

Western blot analysis. Protein levels of m-calpain large subunit and α-tubulin in C_2C_{12} myoblasts and myotubes were measured as described previously (38, 42). Protein concentrations were determined by Bradford's method (9). After the blotted membrane was washed with Tween 20/PBS, reacted bands were detected using horseradish peroxidase-conjugated anti-rabbit or anti-mouse IgG (DAKO, Glostrup, Denmark) with ECL (GE Healthcare Bio-Sciences, Piscataway, NJ).

Calpain activity assay. Both μ- and m-calpain activities in cell extracts were simultaneously measured by casein zymography in a nondenaturing system (35).

Immunofluorescence microscopy. C_2C_{12} myoblasts grown on Lab-Tek II chamber slides (Nalge Nunc International, Rochester, NY) were double-stained with Alexa Fluor 594-labeled phalloidin for actin and FITC-labeled specific antibody to vinculin (26, 38). After being washed with PBS, the specimens were examined with a confocal laser scanning microscope (LSM410, Carl Zeiss, Oberkochen, Germany).

Cell motility assay. C_2C_{12} myoblasts were tested for the ability to move into a denuded area on the culture dish (Nalge Nunc International).

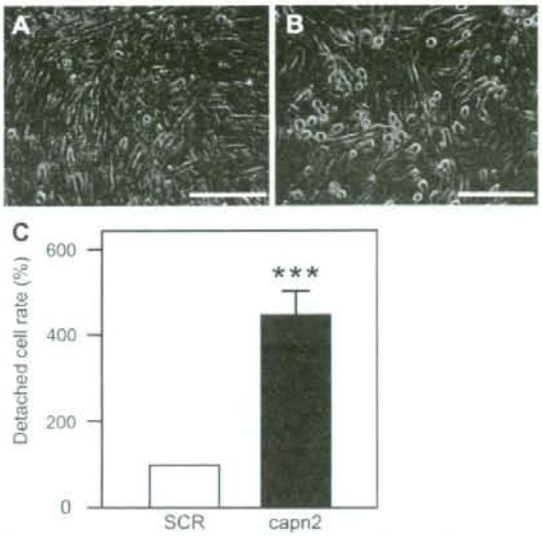

Fig. 3. Facilitation of cell detachment by induction of differentiation in *Capn2* knockdown cells. Ad_shSCR (*A*) and Ad_shcapn2 (*B*) were transfected. The C_2C_{12} cell culture was continued in DMEM containing 10% fetal bovine serum for 3 days up to the confluency. The medium was then replaced by DMEM containing 2% horse serum, and cell differentiation was induced after 3 days. Bar, 150 μm. *C*: relative number of detachment cells per 4 mm^2. Error bars indicate SEs. ***$P < 0.001$ by Student's *t*-test.

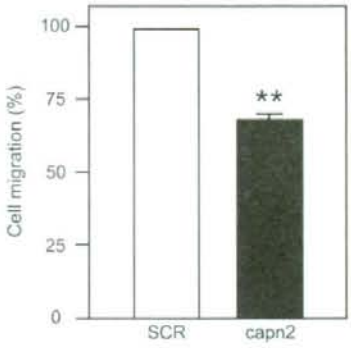

Fig. 5. Reduced migration of myoblasts after adenovirus vector-mediated *Capn2* knockdown. C_2C_{12} cells were transfected with Ad_shSCR or Ad_shcapn2 for 3 days. After 24 h in a quiescent medium, confluent myoblasts were scraped off with a pipette tip, and medium was replaced. The numbers of myoblasts that migrated into the wound site were counted under microscopy. The data represent the average of multiple fields per experiment from 5 separate experiments. Error bar indicates SE. **$P < 0.01$ by Student's *t*-test.

Phase contrast pictures were taken at 0 and 24 h, and the cell migration was determined by the distance moved into the acellular area over time.

Spreading assay. Cell morphology was examined by fluorescent microscopy and optical microscopy, and the number of cells presenting visible cytoplasm or not was determined by visual inspection on Lab-Tek II chamber slides. The rate of spreading was defined as the number of cells with visible cytoplasm/total number of cells × 100 (28).

Statistical analysis. For the quantitative assay, the differences between the Ad_shSCR- and Ad_shcapn2-transfected cells were evaluated by Student's *t*-test. $P < 0.05$ was considered significant.

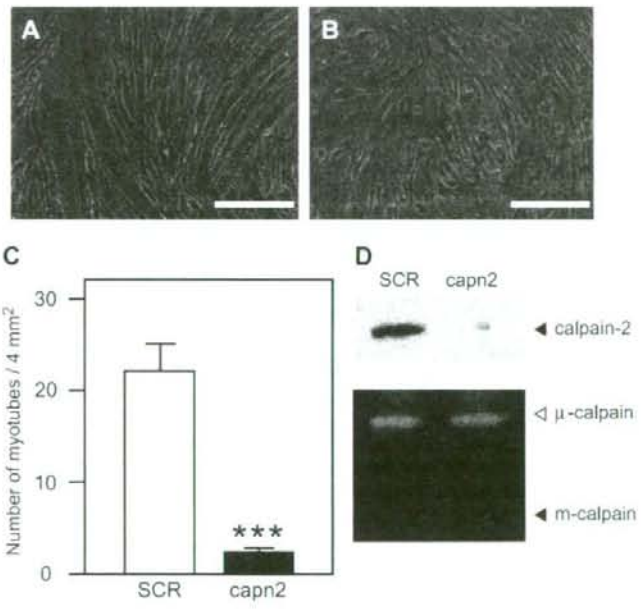

Fig. 4. Inhibition of multinucleated myotubes formation in adenovirus vector-mediated *Capn2* knockdown cells. Three days after transfection, C_2C_{12} myoblasts were reinfected with Ad_shSCR (*A*) or Ad_shcapn2 (*B*), and the medium was replaced by differentiation medium. On *day 7*, these cells were examined with light microscopy. Bar, 150 μm. *C*: the numbers of myotubes in Ad_shSCR and Ad_shcapn2 were counted in 4 mm^2. A myotube was defined as a cell showing at least three nuclei. Error bars indicate SEs. ***$P < 0.001$ by Student's *t*-test. *D*: suppression of *Capn2* on *day 7* after retransfection, analyzed with Western blotting (*top*) or zymography (*bottom*).

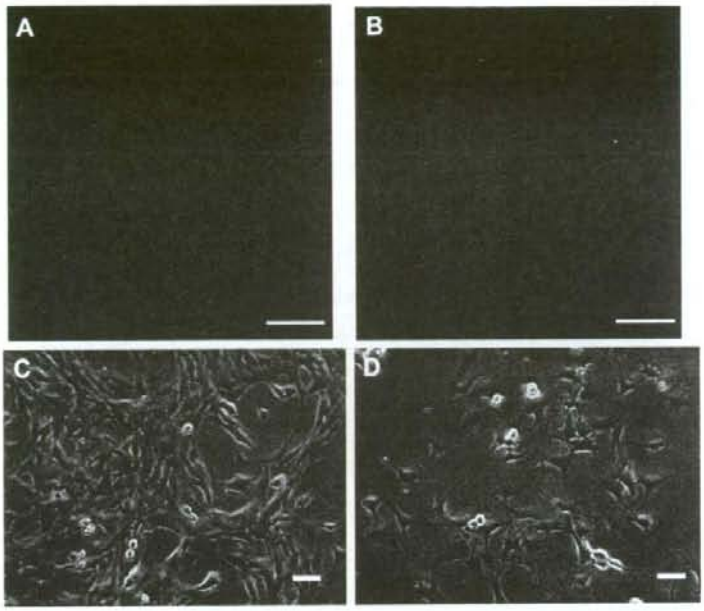

Fig. 6. Morphological characteristics of *Capn2* knockdown cells. At 3 days after the transfection with Ad_shSCR (*A*) or Ad_shcapn2 (*B*), C_2C_{12} myoblasts were plated on the noncoated chamber slide, incubated for 1 h, and stained with Alexa Fluor 594-labeled phalloidin as described in MATERIALS AND METHODS. Ad_shSCR-transfected (*C*) and Ad_shcapn2-transfected (*D*) myoblasts were cultured in GM for 4 days on the noncoated plate, and cells were visualized by light microscopy. Bar, 20 μm.

RESULTS

Expressions of m-calpain large subunit (calpain-2) mRNA and protein during C_2C_{12} myogenesis. To determine the expression level of calpain-2 at different stages of myogenesis, we quantified it at both mRNA and protein levels in mouse C_2C_{12}. Cells were extracted at the subconfluency (*day −1*) and confluency (*day 0*) from the GM cultures and at various stages after the induction of cell differentiation (*days 3-18*) from DM cultures. Although expression levels of *Capn2* mRNA fluctuated slightly at different stages ($P = 0.02–0.04$; Fig. 1*A*), the protein level of full-length calpain-2 showed no significant difference at these stages ($P > 0.05$; Fig. 1, *B* and *C*). No clear correlation was detected between amount of the transcript and the transgene, so the level of calpain-2 protein may be under the influence of posttranslational modifications, folding of the expressed polypeptide, or half-life of the mRNA. We conclude that the protein level of full-length calpain-2 was stable and constitutively expressed in both proliferating and differentiating myoblasts.

Suppression of calpain-2 by adenovirus vector-mediated RNAi in C_2C_{12}. It was difficult to effectively transfect synthetic siRNA or siRNA-expressing plasmids in myoblasts, myotubes, and myocytes. For the complete expression of siRNA to *Capn2* in C_2C_{12} myoblasts, the adenovirus vector was very useful, because the transfection efficiency reached nearly 100% (4). The adenovirus-mediated RNAi was generated by expressing U6 promoter-driven shRNA (Ad_shcapn2), which targets *Capn2*, as well as the control vector with a scrambled sequence (Ad_shSCR). At 3 days after the transfection, C_2C_{12} cells expressing *Capn2*-RNAi showed an apparent reduction of calpain-2 protein level (Fig. 2*A*). To simultaneously assess both activities of μ- and m-calpain in the knockdown cells at 3 days after transfection, casein zymography was carried out. Both enzyme activities were observed in Ad_shSCR-transfected cells, but the knockdown showed only μ-calpain activity with no m-calpain activity (Fig. 2*B*).

Additionally, to assess the continuous reduction of RNAi-mediated calpain-2, we followed the time course of calpain-2 level up to *day 9* after transfection and found that the expressed amount gradually recovered in the posttransfection period (Fig. 2*C*). This reversal may reflect a transient action after the target gene delivery. However, these data demonstrate the potential to suppress calpain-2 with Ad_shcapn2. The activity of calpain-3

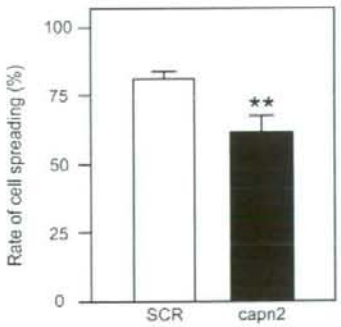

Fig. 7. Reduced spreading of *Capn2* knockdown cells. At 3 days after transfection with Ad_shSCR or Ad_shcapn2, C_2C_{12} myoblasts were plated on the noncoated chamber slides for 3 h. These cells were stained with vinculin antibodies and Alexa Fluor 594-labeled phalloidin as described in MATERIALS AND METHODS. Rates of spreading were measured by determining the ratio of numbers of spreading cells to numbers of total cells. Error bars indicate SEs. $^{**}P < 0.01$ by Student's *t*-test.

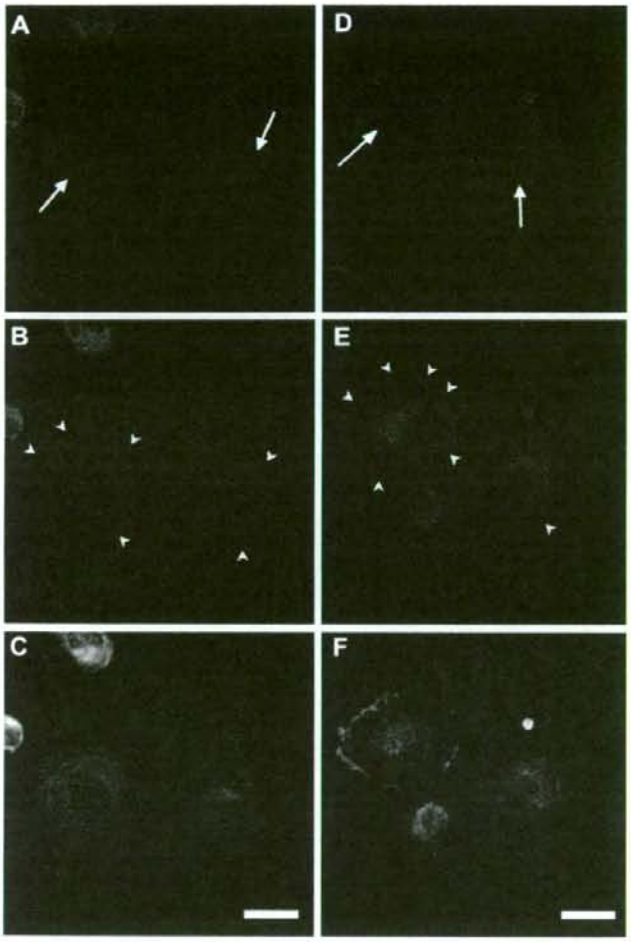

Fig. 8. Loss of central actin stress fiberlike structures (SFLSs). At 5 days after transfection with Ad_shSCR (*A–C*) or Ad_shcapn2 (*D–F*), C_2C_{12} myoblasts were plated on the noncoated chamber slides and incubated for 1 h. Cells were stained with anti-vinculin antibody and Alexa Fluor 594-labeled phalloidin as described in MATERIALS AND METHODS. Arrows and arrowheads indicate SFLSs and focal adhesion, respectively. *A* and *D*, phalloidin; *B* and *E*, vinculin; *C* and *F*, merged. Bar, 20 μm.

specifically contained in skeletal muscle (30) was not detected at all in the current zymography. It should be noted that no compensatory expression of μ-calpain large subunit (calpain-1) was detected during the suppression of calpain-2. The m-calpain activity of cells transfected with Ad_shcapn2 decreased to 5–27% ($P < 0.0005$), compared with that with Ad_shSCR on *days 3* to *7* after the transfection (Fig. 2, *B* and *C*). However, at that time, no significant difference was observed in the activity of μ-calpain between Ad_shSCR and Ad_shcapn2 ($P > 0.05$; Fig. 2*D*). On *day 9* after the transfection, the knockdown efficiency recovered up to 40% and the activity of μ-calpain slightly increased, compared with Ad_shSCR ($P = 0.045$; Fig. 2*D*).

Cell detachment during the differentiation of Capn2 knockdown. Myoblasts were at first grown in GM and then induced to differentiate by switching to DM. The alignment of myoblasts started from *days 3* to *4*, followed by the fusion to multinucleated myotubes between *days 5* and *7*. Previous reports postulated that m-calpain was essential for myoblast differentiation to myotubes via the limited digestion of membrane proteins (25). We examined whether knockdown of *Capn2* inhibits the myoblast fusion and/or differentiation to myotubes. On *day 3* after the transfection when these cells reached the confluency, we started the differentiation. Myoblasts transfected with Ad_shSCR became aligned and started to fuse on *day 3* after the induction of differentiation. However, those cells transfected with Ad_shcapn2 did not fuse (Fig. 3, *A* and *B*). Furthermore, *Capn2* knockdown cells had changed morphology and diminished adhesiveness, resulting in numerous detachments from the dish (Fig. 3*C*).

Inhibition of myoblast fusion to multinucleated myotubes with the selective knockdown of Capn2. Because the duration of adenovirus-vector mediated expression of both the transcript and the transgene is transient, the permanent knockdown is not expected. Actually, the knockdown was restored from *day 7* after the transfection (Fig. 2*C*). For an exact assessment of the inhibitory effect of RNAi, it is necessary for evaluating myoblast differentiation to keep the high knockdown activity. We

Table 1. *Typical phenotypes with inhibition of calpain activities*

Tissue:	Skeletal Muscle						
Cell:	Myoblast					Fibroblast	
Method	RNAi	Calpastatin Overexpression	Pharmacological Inhibitor	Antisense		RNAi	
Target of Calpain:	2	All calpains		1	2	1	2
μ-Calpain activity, %	100	*	*	50	*	40–50	120–130
m-Calpain activity, %	0	*	*	*	50	100	15–30
Typical Phenotype:	↑ Detachment	↓ Myotube formation	↓ Myotube formation	↓ Spreading	↓ Spreading	Unchanged	Morphological change
	↓ Myotube formation			↓ Adhesion	Morphological change		Membrane protrusion
	↓ Migration				↓ Adhesion		
	Morphological change						
	↓ Spreading						
Reference:	Present study	7	6	28	28	19	19

*Data not shown. RNAi, RNA interference; ND, not detected.

repeated the transfection on *day 3* after the initial treatment. Then, we counted the number of myotubes (a myotube was defined as a cell with at least three nuclei).

In control cells on *day 7* in DM, fusion to multinucleated myotubes/myocytes was observed after successive transfection on *day 3* with Ad_shSCR (Fig. 4, *A* and *C*). In contrast, the *Capn*2 knockdown cells showed neither fusion nor differentiation to mature myotubes or myocytes (Fig. 4, *B* and *C*). In addition, there were fewer nuclei and smaller myotubes in Ad_shcapn2-transfected cell cultures compared with the control (Fig. 4, *A* and *B*). Retransfection of the adenovirus vector on *day 3* after the initial transfection prolonged the RNAi action up to *day 7* while maintaining the constant expression of μ-calpain (Fig. 4*D*). Thus, we conclude that the Ad_shcapn2 has strongly inhibited the myoblast fusion and the inhibition was independent of μ-calpain.

Reduced migration and altered morphology after Capn2 knockdown. Calpain-deficient embryonic fibroblasts have been reported not to regulate the membrane protrusion dynamics during fibroblast migration (19, 20). To evaluate whether the specific knockdown of *Capn*2 affects skeletal myoblast migration, we examined cell motility at 3 days after transfection with Ad_shSCR or Ad_shcapn2. Cell movement was analyzed by wound healing assay. An area of a monolayer culture was denuded, and the number of cells that traveled toward the acellular front was measured. Neither protein nor activity levels of m-calpain were observed in the C_2C_{12} cells transfected with Ad_shcapn2 for 3 days (data not shown). These cells showed distinctly reduced migration rates, compared with control cells transfected with Ad_shSCR (Fig. 5), providing evidence that m-calpain makes a significant contribution to cell motility. Morphologically, these knockdown cells transfected with Ad_shcapn2 for 3 days revealed numerous membrane protrusions and filopodia at 1 h after the plating (Fig. 6, *A* and *B*) and maintained the structure up to *day 4* after the transfection (Fig. 6, *C* and *D*).

Disruption of architecture of cytoskeleton during the myoblast spreading. Functional assessment of m-calpain was applied to the myoblast spreading. The C_2C_{12} cells transfected with Ad_shSCR or Ad_shcapn2 for 3 days were plated on the noncoated chamber slides and monitored from 10 min to 3 h. In the control Ad_shSCR-transfected cells, the number of spreading cells gradually increased. In contrast, the cell spreading was delayed in the Ad_shcapn2-transfected cells. A large number of cells kept the round morphology for 3 h. At 3 h after the plating, 80.5 ± 3.9% cells had spread in the control slides. However, *Capn*2 knockdown cells showed a reduced spreading rate (64.3 ± 7.1%; $P < 0.01$, Fig. 7). These results indicated that the defect in spreading was related to the inhibition of m-calpain activity.

Furthermore, the distribution of cytoskeleton in *Capn*2 knockdown cells differed from that of the control cells. To explore whether the knockdown of *Capn*2 affects the cytoskeletal organization, we plated myoblasts transfected with Ad_shSCR or Ad_shcapn2 for 5 days on the chamber slides and observed the cytoskeleton using double-fluorescence microscopy. Actin fibers were visualized with Alexa Fluor 594-labeled phalloidin. Vinculin reported to be hydrolyzed with m-calpain (21) was detected with the specific antibody labeled with FITC (Fig. 8). Ad_shSCR-transfected cells contained numerous stress fiberlike structures (SFLSs) with focal adhesions. However, *Capn*2 knockdown cells lost SFLSs, particularly the central SFLSs (Fig. 8D). We also observed ruffled membranes in the Ad_shcapn2-transfected cells and a loss of vinculin containing focal adhesions at the cell periphery. These findings indicate that m-calpain plays an important role in regulating the localization of actin cytoskeleton and focal adhesion.

DISCUSSION

In the present study, we have generated an in vitro knockdown system for m-calpain to evaluate the physiological effects of decreased m-calpain activity, including muscle-specific differentiation per se from myoblasts to myotubes/myocytes and the general mechanism of cell locomotion via cytoskeletal organization. For the first time, we have demonstrated the following four main results: *1*) selective loss of m-calpain enzyme and, accordingly, its activity; *2*) the strong inhibition of m-calpain with no direct effect on μ-calpain activity; *3*) the ceasing of myoblast development to myotubes and/or myocytes; and *4*) a partial blocking of the locomotion

Table 1.—*Continued*

Pulmonary Artery	Breast	Uterine		Transgenic Mouse			
Endothelial Cells	Breast Cancer Cell	Cervical Cancer Cell					Fibroblast
RNAi	RNAi	RNAi		Knockout			
2	1	1	2	1	2	4	4
100	20–30	Effective reduction	100	0		0	0
40	N.D.	100	Effective reduction	100		0	0
↓ Migration	↓ Migration	Unchanged	Chromosome misalignment	↓ Platelet aggregation	Embryonic lethality	Embryonic lethality	↓ Migration
↓ Proliferation	Morphological change			↓ Clot retraction		×Vasculogenesis	Morphological change
						× Erythropoiesis	
34	46	23	23	2	16	1	15

and proliferation (Fig. S1; the online version of this article contains supplemental data) of myoblasts.

In a wide variety of cells such as fibroblasts, myoblasts, endothelial cells, and cancer cells (1, 2, 6, 7, 15, 16, 19, 23, 28, 34, 46), calpains have been implicated in many aspects of cell physiology, including the cell spreading, migration, and actin remodeling (Table 1). However, the absence of fully specific calpain inhibitors has so far prevented unambiguous proof of a particular role. Previous methods (6, 7, 13, 14, 28) were insufficient for both qualitative and quantitative purposes, i.e., less specific for discriminating each calpain isoform and not completely suppressing the target calpain in a pinpoint manner. Thus, the RNAi strategy, which can inhibit each calpain specifically, would be a powerful tool to clarify physiological functions.

Despite stable expressions of μ- and m-calpain (Figs. 1 and 2), both activities would be increased during the myoblast fusion, concomitantly with myotube formation, and restored after the fusion (8, 11). Balances between μ-calpain and its specific inhibitor, calpastatin, or between m-calpain and calpastatin are assumed to determine their net proteolytic activities, when the proteases and inhibitors are freely accessible to one another. The temporary diminution in calpastatin allows the activation of calpain and calpain-induced proteolysis, which is required for myoblast fusion (5). In addition, other mechanisms such as the posttranslational modification (39), dissociation, and/or translocation from the counterpart (21) may be working for enhancement of the enzyme activity. Furthermore, the expression of μ-calpain was independent of m-calpain, suggesting no cross talk between these isoforms. In the present study, the increase of μ-calpain activity was seen in *Capn*2 knockdown cells, which recovered m-calpain activity up to 40% at 9 days after transfection (Fig. 2*D*). However, no compensation of μ-calpain activity was detectable at 3 days after transfection (Fig. 2*B*) and at 7 days after retransfection (Fig. 4*D*) in *Capn*2 knockdown cells. These data suggest that the expression of μ-calpain is not linked to m-calpain activity. The activation of m-calpain but not μ-calpain is required for induction of the limited proteolysis of membrane proteins that may be closely related to the myoblast fusion. Overall, m-calpain is essential for muscle cell differentiation, especially during the burst of myoblast fusion at the initial stage of differentiation. On the other hand, previous investigations demonstrated that μ-calpain did not affect myoblast fusion (3). Thus, these two isozymes might have distinctly different functions.

Interestingly, the phenomena such as fusion or differentiation to mature myotubes were not seen in filamin C (FLNc) knockdown myoblasts as well as *Capn*2 knockdown myoblasts. FLNc is the muscle-specific member of a family of actin binding proteins. The FLNc knockdown myoblasts display defects in differentiation and fusion ability and ultimately form multinucleated "myoballs" (10). These data indicate that FLNc is critical for normal myogenesis as well as for the maintenance of the structural integrity of the muscle fibers. Although the causal relation of two similar phenomena is not clear, a number of molecules have been implicated in muscle cell differentiation.

Most studies so far lacked a direct proof that m-calpain, but not μ-calpain, is actually working in myogenesis. Considering intracellular physiological Ca^{2+} concentration at submicromolar level (17), m-calpain that requires millimolar Ca^{2+} concentration for the full activation leaves us an exciting challenge in muscle biology. Although treatment by several nonspecific calpain inhibitors has been reported to suppress the progression of muscle diseases (14), the responsible calpain has not been identified. m-Calpain plays an indispensable role in murine embryogenesis, possibly related to preimplantation development (16).

In fibroblasts of the *Capn*4$^{-/-}$ mouse that has lost both μ- and m-calpain, similar morphological change in *Capn*2 knockdown was observed, showing numerous protrusions (15, 19). These *Capn*2 knockdown cells had only μ-calpain activity (data not shown). Protrusion may reflect the polymerization of actin filaments at the barbed ends and their formation of a highly branched dendritic network that drives membrane extension at the leading edge of lamellipodia (32). Huttenlocher's group has indicated that the membrane protrusion is regulated by m-calpain-mediated proteolysis of cortactin in vivo (31, 32). Additionally, cortactin may play a key role in the dynamic

assembly and disassembly in actin polymerization at the cell periphery (45). Cleavage of other cytoskeletal proteins, such as talin, spectrin, and focal adhesion kinase, has been considered to be responsible for abnormal organization of cytoskeleton. The findings of the present study that knockdown of *Capn2* lost SFLSs strongly suggests the involvement of m-calpain among calpain family members in the formation of SFLSs in the myoblasts (33).

Integrin-mediated motility decreased in *Capn4*$^{-/-}$ fibroblasts that lack both μ- and m-calpain (15), and calpain inhibition may negatively modulate cell migration through the inhibition of new adhesions and the destabilization of the cytoskeleton (13). We have observed similarly reduced migration in *Capn2* knockdown cells. Recent investigation demonstrated that channel kinase transient receptor potential melastatin 7 localizes to peripheral adhesion complexes with m-calpain, where it regulates cell adhesion by controlling the protease activity (41). Cell adhesion is regulated through m-calpain by mediating the calcium influx into peripheral adhesion complexes. Thus, m-calpain would play dual roles: *1*) regulation of migration of various kinds of cells and *2*) muscle-specific fusion during differentiation. These functions may be closely related to an invasion or metastasis of cancer cells and to the development of muscle or cardiac diseases in clinical settings, leaving us fascinating problems to be resolved in both basic and clinical sciences.

GRANTS

This work was supported by Riken; Ministry of Education, Culture, and Science Grant; Ministry of Welfare and Labor, Japan; the Fugaku Research Foundation; and the Motor Vehicle Foundation.

REFERENCES

1. **Arthur JS, Elce JS, Hegadorn C, Williams K, Greer PA.** Disruption of the murine calpain small subunit gene, Capn4: calpain is essential for embryonic development but not for cell growth and division. *Mol Cell Biol* 20: 4474–4481, 2000.
2. **Azam M, Andrabi SS, Sahr KE, Kamath L, Kuliopulos A, Chishti AH.** Disruption of the mouse mu-calpain gene reveals an essential role in platelet function. *Mol Cell Biol* 21: 2213–2220, 2001.
3. **Balcerzak D, Poussard S, Brustis JJ, Elamrani N, Soriano M, Cottin P, Ducastaing A.** An antisense oligodeoxyribonucleotide to m-calpain mRNA inhibits myoblast fusion. *J Cell Sci* 108: 2077–2082, 1995.
4. **Bangari DS, Mittal SK.** Current strategies and future directions for eluding adenoviral vector immunity. *Curr Gene Ther* 6: 215–226, 2006.
5. **Barnoy S, Glaser T, Kosower NS.** Calpain and calpastatin in myoblast differentiation and fusion: effects of inhibitors. *Biochim Biophys Acta* 1358: 181–188, 1997.
6. **Barnoy S, Kosower NS.** Caspase-1-induced calpastatin degradation in myoblast differentiation and fusion: cross-talk between the caspase and calpain systems. *FEBS Lett* 546: 213–217, 2003.
7. **Barnoy S, Maki M, Kosower NS.** Overexpression of calpastatin inhibits L8 myoblast fusion. *Biochem Biophys Res Commun* 332: 697–701, 2005.
8. **Barnoy S, Supino-Rosin L, Kosower NS.** Regulation of calpain and calpastatin in differentiating myoblasts: mRNA levels, protein synthesis and stability. *Biochem J* 351: 413–420, 2000.
9. **Bradford MM.** A rapid and sensitive method for the quantitation of microgram quantities of protein utilizing the principle of protein-dye binding. *Anal Biochem* 72: 248–254, 1976.
10. **Dalkilic I, Schienda J, Thompson TG, Kunkel LM.** Loss of FilaminC (FLNc) results in severe defects in myogenesis and myotube structure. *Mol Cell Biol* 26: 6522–6534, 2006.
11. **Dargelos E, Dedieu S, Moyen C, Poussard S, Veschambre P, Brustis JJ, Cottin P.** Characterization of the calcium-dependent proteolytic system in a mouse muscle cell line. *Mol Cell Biochem* 231: 147–154, 2002.
12. **Dayton WR, Goll DE, Zeece MG, Robson RM, Reville WJ.** A Ca^{2+}-activated protease possibly involved in myofibrillar protein turnover. Purification from porcine muscle. *Biochemistry* 15: 2150–2158, 1976.
13. **Dedieu S, Poussard S, Mazeres G, Grise F, Dargelos E, Cottin P, Brustis JJ.** Myoblast migration is regulated by calpain through its involvement in cell attachment and cytoskeletal organization. *Exp Cell Res* 292: 187–200, 2004.
14. **Donkor IO.** A survey of calpain inhibitors. *Curr Med Chem* 7: 1171–1188, 2000.
15. **Dourdin N, Bhatt AK, Dutt P, Greer PA, Arthur JS, Elce JS, Huttenlocher A.** Reduced cell migration and disruption of the actin cytoskeleton in calpain-deficient embryonic fibroblasts. *J Biol Chem* 276: 48382–48388, 2001.
16. **Dutt P, Croall DE, Arthur SC, De Veyra T, Williams K, Elce JS, Greer PA.** m-Calpain is required for preimplantation embryonic development in mice. *BMC Dev Biol* 6: 3, 2006.
17. **Ebashi S, Nonomura Y, Toyo-oka T, Katayama E.** Regulation of muscle contraction by the calcium-troponin-tropomyosin system. In: *Calcium in Biological Systems: Symposia of the Society for Experimental Biology no. 30*, edited by Duncan CJ. New York: Cambridge Univ. Press, 1976, p. 349–360.
18. **Elbashir SM, Harborth J, Lendeckel W, Yalcin A, Weber K, Tuschl T.** Duplexes of 21-nucleotide RNAs mediate RNA interference in cultured mammalian cells. *Nature* 411: 494–498, 2001.
19. **Franco S, Perrin B, Huttenlocher A.** Isoform specific function of calpain 2 in regulating membrane protrusion. *Exp Cell Res* 299: 179–187, 2004.
20. **Franco SJ, Huttenlocher A.** Regulating cell migration: calpains make the cut. *J Cell Sci* 118: 3829–3838, 2005.
21. **Goll DE, Thompson VF, Li H, Wei W, Cong J.** The calpain system. *Physiol Rev* 83: 731–801, 2003.
22. **Hartley DP, Klaassen CD.** Detection of chemical-induced differential expression of rat hepatic cytochrome P450 mRNA transcripts using branched DNA signal amplification technology. *Drug Metab Dispos* 28: 608–616, 2000.
23. **Honda S, Marumoto T, Hirota T, Nitta M, Arima Y, Ogawa M, Saya H.** Activation of m-calpain is required for chromosome alignment on the metaphase plate during mitosis. *J Biol Chem* 279: 10615–10623, 2004.
24. **Huang J, Forsberg NE.** Role of calpain in skeletal-muscle protein degradation. *Proc Natl Acad Sci USA* 95: 12100–12105, 1998.
25. **Kaur H, Sanwal BD.** Regulation of the activity of a calcium-activated neutral protease during differentiation of skeletal myoblasts. *Can J Biochem* 59: 743–747, 1981.
26. **Kawada T, Nakazawa M, Nakauchi S, Yamazaki K, Shimamoto R, Urabe M, Nakata J, Hemmi C, Masui F, Nakajima T, Suzuki J, Monahan J, Sato H, Masaki T, Ozawa K, Toyo-oka T.** Rescue of hereditary form of dilated cardiomyopathy by rAAV-mediated somatic gene therapy: amelioration of morphological findings, sarcolemmal permeability, cardiac performances, and the prognosis of TO-2 hamsters. *Proc Natl Acad Sci USA* 99: 901–906, 2002.
27. **Lebart MC, Benyamin Y.** Calpain involvement in the remodeling of cytoskeletal anchorage complexes. *FEBS J* 273: 3415–3426, 2006.
28. **Mazeres G, Leloup L, Daury L, Cottin P, Brustis JJ.** Myoblast attachment and spreading are regulated by different patterns by ubiquitous calpains. *Cell Motil Cytoskeleton* 63: 193–207, 2006.
29. **McCaffrey AP, Meuse L, Pham TT, Conklin DS, Hannon GJ, Kay MA.** RNA interference in adult mice. *Nature* 418: 38–39, 2002.
30. **Ono Y, Kakinuma K, Torii F, Irie A, Nakagawa K, Labeit S, Abe K, Suzuki K, Sorimachi H.** Possible regulation of the conventional calpain system by skeletal muscle-specific calpain, p94/calpain 3. *J Biol Chem* 279: 2761–2771, 2004.
31. **Perrin BJ, Amann KJ, Huttenlocher A.** Proteolysis of cortactin by calpain regulates membrane protrusion during cell migration. *Mol Biol Cell* 17: 239–250, 2006.
32. **Pollard TD, Borisy GG.** Cellular motility driven by assembly and disassembly of actin filaments. *Cell* 112: 453–465, 2003.
33. **Potter DA, Tirnauer JS, Janssen R, Croall DE, Hughes CN, Fiacco KA, Mier JW, Maki M, Herman IM.** Calpain regulates actin remodeling during cell spreading. *J Cell Biol* 141: 647–662, 1998.
34. **Qiu K, Su Y, Block ER.** Use of recombinant calpain-2 siRNA adenovirus to assess calpain-2 modulation of lung endothelial cell migration and proliferation. *Mol Cell Biochem* 292: 69–78, 2006.
35. **Raser KJ, Posner A, Wang KK.** Casein zymography: a method to study mu-calpain, m-calpain, and their inhibitory agents. *Arch Biochem Biophys* 319: 211–216, 1995.
36. **Riazi AM, Lee H, Hsu C, Van Arsdell G.** CSX/Nkx2.5 modulates differentiation of skeletal myoblasts and promotes differentiation into neuronal cells in vitro. *J Biol Chem* 280: 10716–10720, 2005.

37. **Russell WC.** Update on adenovirus and its vectors. *J Gen Virol* 81: 2573–2604, 2000.
38. **Sakamoto A, Ono K, Abe M, Jasmin G, Eki T, Murakami Y, Masaki T, Toyo-oka T, Hanaoka F.** Both hypertrophic and dilated cardiomyopathies are caused by mutation of the same gene, delta-sarcoglycan, in hamster: an animal model of disrupted dystrophin-associated glycoprotein complex. *Proc Natl Acad Sci USA* 94: 13873–13878, 1997.
39. **Salamino F, Averna M, Tedesco I, De Tullio R, Melloni E, Pontremoli S.** Modulation of rat brain calpastatin efficiency by post-translational modifications. *FEBS Lett* 412: 433–438, 1997.
40. **Sorimachi H, Ishiura S, Suzuki K.** Structure and physiological function of calpains. *Biochem J* 328: 721–732, 1997.
41. **Su LT, Agapito MA, Li M, Simonson WT, Huttenlocher A, Habas R, Yue L, Runnels LW.** TRPM7 regulates cell adhesion by controlling the calcium-dependent protease calpain. *J Biol Chem* 281: 11260–11270, 2006.
42. **Takahashi M, Tanonaka K, Yoshida H, Oikawa R, Koshimizu M, Daicho T, Toyo-oka T, Takeo S.** Effects of ACE inhibitor and AT1 blocker on dystrophin-related proteins and calpain in failing heart. *Cardiovasc Res* 65: 356–365, 2005.
43. **Toyo-oka T, Kawada T, Nakata J, Xie H, Urabe M, Masui F, Ebisawa T, Tezuka A, Iwasawa K, Nakajima T, Uehara Y, Kumagai H, Kostin S, Schaper J, Nakazawa M, Ozawa K.** Translocation and cleavage of myocardial dystrophin as a common pathway to advanced heart failure: a scheme for the progression of cardiac dysfunction. *Proc Natl Acad Sci USA* 101: 7381–7385, 2004.
44. **Toyo-oka T, Shimizu T, Masaki T.** Inhibition of proteolytic activity of calcium activated neutral protease by leupeptin and antipain. *Biochem Biophys Res Commun* 82: 484–491, 1978.
45. **Weaver AM, Karginov AV, Kinley AW, Weed SA, Li Y, Parsons JT, Cooper JA.** Cortactin promotes and stabilizes Arp2/3-induced actin filament network formation. *Curr Biol* 11: 370–374, 2001.
46. **Wu M, Yu Z, Fan J, Caron A, Whiteway M, Shen SH.** Functional dissection of human protease mu-calpain in cell migration using RNAi. *FEBS Lett* 580: 3246–3256, 2006.
47. **Xia H, Mao Q, Paulson HL, Davidson BL.** siRNA-mediated gene silencing in vitro and in vivo. *Nat Biotechnol* 20: 1006–1010, 2002.
48. **Yoshida H, Takahashi M, Koshimizu M, Tanonaka K, Oikawa R, Toyo-oka T, Takeo S.** Decrease in sarcoglycans and dystrophin in failing heart following acute myocardial infarction. *Cardiovasc Res* 59: 419–427, 2003.
49. **Yu JY, DeRuiter SL, Turner DL.** RNA interference by expression of short-interfering RNAs and hairpin RNAs in mammalian cells. *Proc Natl Acad Sci USA* 99: 6047–6052, 2002.
50. **Zatz M, Starling A.** Calpains and disease. *N Engl J Med* 352: 2413–2423, 2005.